Appl Biochem Biotechnol (2010) 160:2148–2165
DOI 10.1007/s12010-009-8734-5

Evaluation of Immobilized Metal-Ion Affinity Chromatography (IMAC) as a Technique for IgG_1 Monoclonal Antibodies Purification: The Effect of Chelating Ligand and Support

I. T. L. Bresolin · M. Borsoi-Ribeiro · W. M. S. C. Tamashiro · E. F. P. Augusto · M. A. Vijayalakshmi · S. M. A. Bueno

Received: 13 March 2009 / Accepted: 28 July 2009 /
Published online: 23 August 2009

Abstract Monoclonal antibodies (MAbs) have been used for therapies and some analytical procedures as highly purified molecules. Many techniques have been applied and studied, focusing on monoclonal antibodies purification. In this study, an immobilized metal affinity chromatography membrane was developed and evaluated for the purification of anti-TNP IgG_1 mouse MAbs from cell culture supernatant after precipitation with a 50% saturated ammonium sulfate solution. The chelating ligands iminodiacetic acid, carboxymethylated aspartic acid (CM-Asp), nitrilotriacetic acid, and tris (carboxymethyl) ethylenediamine in agarose gels with immobilized Ni(II) and Zn(II) ions were compared for the adsorption and desorption of MAbs. The most promising chelating ligand—CM-Asp—was then coupled to poly(ethylene vinyl alcohol) (PEVA) hollow fiber membranes. According to SDS-PAGE and ELISA analyses, a higher selectivity and a purification factor of 85.9 (fraction eluted at 500 mM Tris) were obtained for IgG_1 using PEVA-CM-Asp-Zn(II). The anti-TNP MAb could be eluted under mild pH conditions causing no loss of antigen binding capacity.

Keywords Monoclonal antibodies · Purification · Adsorption · IMAC · Affinity membrane · Downstream processing

I. T. L. Bresolin · M. Borsoi-Ribeiro · S. M. A. Bueno (✉)
School of Chemical Engineering, University of Campinas, UNICAMP, P.O. Box 6066,
13083-970 Campinas, SP, Brazil
e-mail: sonia@feq.unicamp.br

W. M. S. C. Tamashiro
Institute of Biology, University of Campinas, UNICAMP, P.O. Box 6109, 13083-970 Campinas,
SP, Brazil

E. F. P. Augusto
Institute for Technological Research of the State of São Paulo, Av. Prof. Almeida Prado, 532,
05508-901 Sao Paulo, SP, Brazil

M. A. Vijayalakshmi
Centre for Bioseparation Technology, VIT University Vellore, Vellore 632 014, Tamil Nadu, India

Introduction

Monoclonal antibodies (MAb) are monospecific antibodies with extremely high selectivity and sensitivity in the recognition of the antigens against which they are developed. Large amounts of MAbs have been commercially produced by culturing hybridoma cells in mammalian bioreactor systems [1, 2]. Nowadays, due to the use of genomics and proteomics, many technical efforts have been made for the development of a second generation of MAbs with better affinities, decreased immunogenicity, and optimized effector functions [3].

Due to their main application being in clinical and diagnostic areas, MAbs of high purity are required. Therefore, many techniques have been studied [4–8]. MAbs are usually recovered from complex media (ascitic fluid or cell-culture supernatant) composed of amino acids, proteins, and cells. After cell removal using unit operations such as centrifugation and filtration, chromatographic techniques based on ion exchange, size exclusion, hydrophobic interaction, and affinity principles are used in the final purification processes aiming at the elimination of impurities [9].

Biospecific ligands, such as protein A or G, have been widely used due to their high affinity for the Fc antibody domain. However, they are characterized by low capacity, low chemical and proteolytic stability, high costs, and drastic elution conditions which may cause loss of MAb activity [10]. As an alternative, pseudobiospecific ligands have been under development for antibodies purification [10–14].

Immobilized metal-ion affinity chromatography (IMAC), a group-specific affinity technique for separating proteins, is based on the reversible interaction between various amino acid side chains and immobilized metal ions [15]. This technique has shown promising results for purification of different species and subclass of antibodies from different sources [16–24]. In IMAC, chelating ligands play an important role due to the presence of electron donor atoms in their structure which are able to bind metal ions forming metal chelates [25, 26]. The choice of chelating ligand must be made focusing on the stability of the metal ion complex and the availability of free coordination sites for protein binding. The most used chelating ligand is tridentade iminodiacetic acid (IDA). Tetradentades, like carboxymethylated aspartic acid (CM-Asp) and nitrilotriacetic acid (NTA), and pentadentades such as Tris (carboxymethyl) ethylenediamine (TED) contain fewer free sites to bind the protein, which can make them more selective in the purification process. Figure 1 shows the schematic structures of IDA, CM-Asp, NTA, and TED chelating ligands.

The most common support materials used in affinity chromatography are soft gels. However, performance is limited by mass transfer due to compressibility and pore diffusion. As an alternative, the idea of using microporous membranes as support matrices for affinity separation has been introduced, since they provide higher flow rates, much lower pressure drops, easier scale-up, mechanical stability, and higher productivities [27, 28].

In a recent study, Serpa and colleagues [18] evaluated the effect of four metal ions (Cu (II), Ni(II), Zn(II), and Co(II)) immobilized onto an IMAC affinity hollow fiber membrane system—an IDA covalently linked poly(ethylenevinyl alcohol) membrane, called IDA-PEVA—for purification of anti-TNP IgG_1 mouse MAbs, which were efficiently adsorbed and eluted while maintaining their antigenic properties. However, a systematic investigation of different IMAC-chelating agents used for MAb purification is still of paramount relevance. The present work extends the application of Serpa and coworkers' studies of anti-TNP IgG_1 mouse MAb purification [18] in order to obtain fundamental data for the

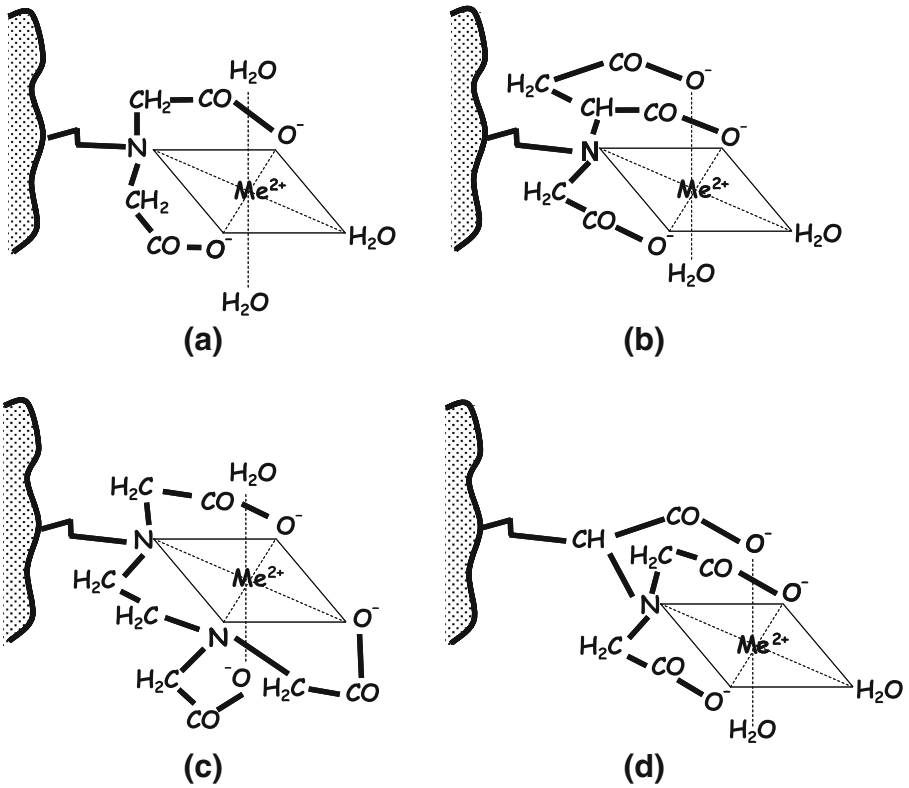

Fig. 1 Schematic structures of different chelate ligand immobilized metal ions having a coordination number of 6. **a** IDA; **b** CM-Asp; **c** TED; **d** NTA

development of large-scale MAb purification processes in IMAC membrane chromatography with Ni(II) and Zn(II). The selection of chelating agents aimed to study the effect of tridentade (IDA), tetradentades (NTA, CM-Asp), and pentadentade (TED) on the selectivity for MAb purification using agarose gel. Studies with PEVA membranes as support material were performed with the most selective chelating ligand (CM-Asp), including a binding study with adsorption isotherm data analyzed using the Langmuir, Langmuir–Freundlich, and Temkin models. The breakthrough curves were useful for determining the dynamic capacity of the affinity membrane since they are the basis for Mab purification process design, scale-up, and optimization.

Materials and Methods

Materials

The agarose gel (Sepharose® 6B) and the high molecular weight marker for sodium dodecyl sulfate-polyacrylamide gel electrophoresis (SDS-PAGE; myosine, 212 kDa; α2-macroglobulin, 170 kDa; β-galactosidase, 116 kDa; transferrin, 76 kDa; glutamic dehydrogenase, 53 kDa) were purchased from GE Healthcare (USA). Iminodiacetic acid

(IDA), L-aspartic acid (Asp), ammonium persulphate and epichlorohydrin were purchased from Sigma (USA). Tris(hydroxyethyl amino methane) (Tris), disodium ethylenediamine-tetraacetic acid (EDTA), nickel, zinc, and ammonium sulfate were purchased from Merck (Germany). For SDS-PAGE analysis, acrylamide, bis-acrylamide, SDS, and dithiotrietol were purchased from BioRad (USA). All other chemicals were of analytical grade. Milli-Q water (Millipore, USA) was used to prepare all buffers and solutions.

The poly(ethylenevinyl alcohol)-PEVA-hollow fiber cartridges (Model Eval 4A, 1 m^2 surface area) were purchased from Kuraray (Japan). The hollow fiber had an internal diameter of 200 μm, a wall thickness of 20 μm, and a nominal molecular mass cutoff of 600 kDa.

MAb

Anti-TNP MAb, isotype IgG_1, expressed by the hybridoma 1B2.1B6 [29], was produced in vitro in a 500-mL spinner flask (Bellco Micro Carrier, USA), using Dulbecco's Modified Eagle's culture media (Sigma, USA) enriched with 10% bovine fetal serum (Nutricell, Brazil). The cells were removed from the cultures by centrifugation, and the material was then filtered through a 0.22-μm cellulose membrane (Millipore, USA).

Affinity Gels

Agarose (Sepharose-6B) activation with epichlorohydrin and coupling to IDA were carried out as described in the literature [16–18, 22]. Agarose-NTA and agarose-TED gels were purchased from Sigma (USA).

The synthesis of agarose-CM-Asp gel followed two steps: first, the coupling of L-aspartic acid to epichlorohydrin activated gel and then the carboxymethylation reaction, via nitrogen of Asp [30]. Twenty grams of suction-dried activated Sepharose-6B was washed with ultrapure water, suction-dried, and transferred to a becker. Five grams of L-aspartic acid was added to a 50-mL $NaHCO_3/Na_2CO_3$ 1.0 mol L^{-1} pH11.5 solution. The reaction mixture was brought to about 80 °C for 4 h and allowed to cool to room temperature overnight in orbital agitation. The gel was collected by filtration, washed ten times with ultrapure water, and transferred to a becker; 12.6 g of bromoacetic acid was added to 30 mL NaOH 4.0 mol L^{-1} solution, and the pH was adjusted to 10.5. This solution was added to L-aspartic coupled gel and maintained in orbital agitation overnight at room temperature. The gel was collected by filtration and washed continuously with ultrapure water until the pH reached about 6.0.

Immobilization of CM-Asp on a PEVA Hollow Fiber Membrane

Cut Membrane Derivatization

A commercial PEVA hollow fiber cartridge was disassembled, and the fibers were removed and finely cut into pieces of around 2 mm in length. The cut PEVA membranes were activated with epichlorohydrin [18, 22, 31], and CM-Asp was coupled to them as described for agarose gel.

Minicartridge Derivatization

A small-scale cartridge of PEVA hollow fibers was manufactured using fibers from an available commercial cartridge. As indicated above, the fibers were cut and assembled in a

minicartridge with an effective length of 4.5 cm. The amount of fibers in this cartridge was 0.14 g (dry mass) with a surface area of 71.6 cm^2 and a bed volume of 0.16 cm^3 [18]. The PEVA hollow fiber cartridge was activated with epichlorohydrin, and CM-Asp was coupled to it by recirculation of the solutions (epichlorohydrin, L-aspartic acid in $NaHCO_3/Na_2CO_3$ 1.0 mol L^{-1} pH 11.5 and bromoacetic acid in NaOH 4.0 mol L^{-1}) inside the fibers using a peristaltic pump.

Cell Culture Supernatant Precipitation and Dialysis

Following the procedure presented by El-Kak and Vijayalakshmi [32], 200 mL of cell culture supernatant was precipitated with 200 mL of ammonium sulfate saturated solution (50% saturation final solution). The ammonium sulfate solution was slowly poured into the cell culture supernatant; the solution was stirred for 1 h and then centrifuged at 3,000×*g* for 30 min. The precipitate was dissolved in Tris–HCl 50 mM, pH 7.0, and dialyzed against the same buffer for 30 h. All steps were carried out at 4 °C.

Chromatographic Procedures

Chromatographic procedures were carried out aiming to determine the elution profile of the proteins in Tris–HCl 50 mM, pH 7.0 buffer with Zn(II) and Ni(II) immobilized in different chelating ligands in agarose gel and PEVA hollow fiber membranes. Agarose gels were packed into a column (10 cm × 10 mm I.D.) to give a bed volume varying from 1.0 to 2.0 mL (0.3 to 0.7 g dry gel) depending on the gel. Finely cut PEVA membranes were packed into a column (20 cm × 10 mm I.D.) to give a bed volume of 5.0 mL (1.25 g dry membrane). IMAC gels and membranes were loaded with Ni(II) and Zn(II) from 50 mM sulfate solutions.

Cell culture supernatant precipitated and dialyzed samples containing anti-TNP IgG_1 MAbs were fed into the columns at a flow rate of 0.5 mL/min. Chromatographic procedures were carried out with the ProTech Biochromatography System (Gilson, France). The outlet stream was connected to an absorbance monitor (280 nm) and then to a fraction collector (fractions between 3.0 and 5.0 mL). The adsorption buffer Tris–HCl 25 mM (or 50 mM), pH 7.0 was used, and the retained proteins were eluted with a step increase in Tris concentration ranging from 50 to 700 mM. The column was regenerated with EDTA 50 mM solution, pH 6.5. The fractions were analyzed by the Bradford method [33], those in the protein peaks were analyzed by SDS-PAGE, and IgG_1 was quantified by enzyme-linked immunosorbent assay (ELISA).

Protein Adsorption Studies

Adsorption experiments (stirred tank batch adsorption) for isotherm determination were carried out using prepurified IgG_1 MAbs at 25 °C. The PEVA-CM-Asp-Zn(II) finely cut fibers (10.0 mg dry mass) were weighed in 1.5 mL Eppendorf tubes. The cut fibers were equilibrated with Tris–HCl 50 mM, pH 7.0 for 15 min. Then, aliquots of 1.0 mL of 0.5 to 6.0 mg/mL IgG_1 solutions were added to the Eppendorf tubes, using IgG_1 (purified by agarose-protein G) diluted with adsorption buffer. The tubes were rotated end over end at 6 rpm for 3 h to allow equilibrium to be established. Then, the supernatant was removed, and the unbound protein concentration in the liquid phase was determined by the Bradford method [33]. The adsorbed IgG_1 (q^*) was determined as the difference between the amount of IgG_1 added and that present in the liquid phase after equilibrium (c^*) divided by the dry mass of the adsorbent. Plotting q^* against c^* yielded the equilibrium isotherm. The

parameters of the Langmuir, Langmuir–Freundlich, and Temkin models (Table 1) were fitted to the experimental data employing the iterative fitting method of Levenberg–Marquardt, using Statistica® (Statsoft, USA).

IgG_1 Precipitate Solution Cross-flow Filtration in the PEVA-CM-Asp-Zn(II) Hollow Fiber Cartridge

This experiment was carried out at 25°C with a ProTech Biochromatography System (Gilson, France). Prior to the experiments, the equilibration buffer (Tris–HCl 50 mM, pH 7.0) was pumped through the PEVA-CM-Asp-Zn(II) minicartridge for 15 min in dead-end mode at an inlet flow rate of 1.0 mL/min. A feedstream of IgG_1 precipitate solution (40 mL) at 6.4 mg/mL (total protein) was pumped through the minicartridge in a cross-flow mode in open loop at an inlet flow rate of 0.5 mL/min. The constant inlet flow rate (Q_i) and filtrate flow rate (Q_F) were provided by two peristaltic pumps which maintained the Q_F/Q_i ratio at 0.50. The filtrate outlet passed through the UV detector to monitor the absorbance at 280 nm (protein breakthrough determination). After loading the IgG_1 precipitate solution, unretained proteins were washed out with Tris–HCl 50 mM, pH7.0. Four washing steps in different modes were used: cross-flow filtration, lumen, shell, and backflushing [18, 31]. The retained proteins were eluted in the backflushing mode with a discontinuous step gradient (100–700 mM of Tris–HCl buffer, pH7.0). The effluents were monitored by measuring the absorbance at 280 nm. After elution was completed, the cartridge was sequentially washed in the frontal mode with EDTA 50 mM, pH6.5 and with the loading buffer to restore it to its initial conditions for storage.

Protein concentrations in retained and nonretained fractions were determined by the Bradford method [33] and analyzed by SDS-PAGE under nonreducing conditions. The breakthrough curve was plotted as the ratio of total protein concentration (C) in the filtrate and retentate to that in the feed stream (C_o) as a function of the volume of protein solution throughout.

Analytical Methods

Protein Quantification

The total protein concentration of the fractions collected in the chromatographic runs was quantified by the Bradford method [33], using bovine serum albumin as reference protein.

SDS-PAGE

Fractions of chromatographic peaks were analyzed by SDS-PAGE under denaturating and nonreducing conditions [34] in a Mini-Protean III system (BioRad, USA). The separation

Table 1 Isotherm adsorption models.

Model	Equation	References
Langmuir	$q^* = \frac{q_m C^*}{(K_d + C^*)}$	[18]
Langmuir–Freundlich	$q^* = \frac{q_m (C^*)^n}{K_{d(LF)} + (C^*)^n}$	[41, 42]
Temkim	$q^* = q_T \ln(1 + K_T c^*)$ $K_T = \exp(-\Delta G_{max}/RT)$	[39, 40]

was carried out at 180 V in 7.5% separation gels with a 4% stacking gel. Protein bands were developed by silver staining [35].

Isoelectric focusing

To determine the pI of eluted MAb samples, isoelectric focusing (IEF) analysis were carried out using a PhastSystem (Pharmacia, Sweden) in a pH3–9 gradient polyacrylamide gel (PhastGel IEF 3-9, GE Healthcare, USA). The gel was stained with silver nitrate in accordance with the methods provided by the manufacturer.

Native PAGE

Aiming to evaluate the homogeneity of eluted MAb, a native PAGE was carried out in a PhastSystem (Pharmacia, Sweden) in a 7.5% polyacrylamide gel (PhastGel Homogeneous 7.5, GE Healthcare, USA). The gel was silver-stained according to the methods provided by the manufacturer.

Immunoblotting

After SDS-PAGE run, MAb samples were transferred to a nitrocellulose membrane in a Mini Transblotting III System (Bio-Rad, USA) as described by Towbin et al. [36]. An anti-mouse IgG (Fab specific) antibody conjugated to peroxidase produced in goat (Sigma, USA) was used as secondary antibody. The MAb bands were revealed using a cromogene solution (0.003% H_2O_2, 1 mg/mL 3,3′-diaminobenzidine in Tris–HCl 50 mM, pH7.4).

IgG_1 Quantification and Titulation by ELISA

MAb concentration and activity were determined by solid-phase ELISA as described in the literature [18, 29]. Polyclonal mouse IgG (Sigma, USA) was used as standard protein.

Determination of the Amount of Immobilized Ni(II) and Zn(II)

The metal-loaded columns (agarose and finely cut PEVA membranes) and PEVA membrane minicartridge were washed with 10 column volumes of Tris–HCl 50 mM, pH7.0 followed by elution with EDTA 50 mM, pH6.5. The total amount of Ni(II) and Zn(II) in the eluate was determined by a Perkin Elmer AA100 (USA) atomic absorption spectrophotometer.

Results and Discussion

Chelating Ligand and Metal-Ion Selection for IgG_1 Purification

In order to select the best adsorption center (chelating ligand and metal ion) for IgG_1 purification, preliminary adsorption experiments were performed in gels since their adsorption capacity is higher than that of membranes. The metal ions Ni(II) and Zn(II) were used and chelated to IDA, CM-Asp, TED, and NTA ligands immobilized on agarose gel. The adsorption was performed in the presence of Tris buffer and the elution by addition of Tris up to 700 mM (discontinuous step gradient). Tris buffer is considered a weak

competitive agent in IMAC. Its presence in adsorption may favor a higher selectivity; concentration can be increased in the elution step [18].

The total protein concentration in the feed solution ranged from 10.9 to 23.5 mg/mL, of which approximately 7% corresponded to IgG_1 (obtained by ELISA). Different adsorption centers affected the adsorption and elution of IgG_1 differently. The adsorbent selectivities were determined using SDS-PAGE, as shown in Figs. 2a–d and 3a–d. The total protein mass balances for all chromatographic experiments are shown in Table 2.

In the case of hexa-coordinated metal ions (such as Ni(II) and Zn(II)), IDA has been the chelating ligand most frequently used in IMAC due to its tridentade configuration which chelates the metal ion occupying three coordination sites, leaving the other three sites free for interaction with the protein [25, 26]. The results show adsorption capacities of 4.39 and 3.30 mg/g of dry gel for agarose-IDA-Ni(II) and agarose-IDA-Zn(II), respectively. Nevertheless, the selectivity achieved was not satisfactory, according to SDS-PAGE shown in Fig. 2a, b. Significant amounts of albumin remained adsorbed in both agarose-IDA-Ni(II) and agarose-IDA-Zn(II), corroborating the results presented by Serpa and coworkers [18].

In order to increase selectivities, the tetradendate ligands CM-Asp and NTA and the pentadentade TED were evaluated. The main characteristic of higher dentate ligands is that fewer sites are available for interaction with the protein, and more stable chelates are obtained [25].

According to the results, higher selectivities but lower adsorption capacities were achieved (than with agarose-IDA). When agarose-CM-Asp-Zn(II) was used, for instance, a MAb purity of 77% and a purification factor of 15.5 (Tris–HCl 100 mM elution), determined by ELISA (data not shown), were reached (0.78 mg of total protein/g dry gel).

When NTA was used as the chelating ligand, different selectivities were achieved. Both chelating ligands CM-Asp and NTA chelate the metal ion using three oxygen atoms and just one nitrogen atom. According to the SDS-PAGE in Figs. 2c, d and 3c, d, the selectivity of agarose-CM-Asp was better than that of agarose-NTA (for both Ni(II) and Zn(II)), probably due to the spatial arrangement of CM-Asp atoms [25].

When Ni(II) and Zn(II), chelated to the pentadentade TED, were used, completely different results were achieved. Agarose-TED-Ni(II), for instance, showed a good selectivity (with small amounts of albumin adsorbed, as shown using SDS-PAGE in Fig. 3a) and an adsorption capacity similar to that of CM-Asp-Zn(II) (0.70 mg/g of dry gel). On the other hand, it was expected that zinc immobilized on TED would have a capacity lower than the value observed in this work (3.15 mg/g of dry gel). Nevertheless, Chaga and coworkers [37] discussed the possibility that one or more coordination bonds between the chelating ligand TED and Zn(II) may not be used for the immobilization of this ion. Thus, Zn(II) would make available other coordination sites for interaction with the protein, increasing the capacity of the TED–Zn(II) complex to adsorb proteins, which was observed in the experiments conducted in this work.

Haile and Beidler [38] described a histidine-rich region in the third constant domain of heavy chain (CH3) of murine IgG_1 and humanized murine IgG_1 as a probably site of metal interaction. The authors noted that this domain was conserved among several immunoglobulin species and subclass of human, murine, guinea pig, and rabbit as the specific binding site for metal chelate. Corroborating Hale and Beidler results, Todorova-Balvay and coworkers [13] using computer calculations of accessible surface area of His residues of Fc domain of human IgG_1 (performed using XPLOR) showed that the more probable His 433-x-His 435 sequence presented in the CH3 domain of human IgG heavy chain.

Due to the high selectivity achieved by Ni(II) and Zn(II) chelated to CM-Asp (Fig. 2c, d), PEVA membranes were used as support material, since higher productivities rather than poor adsorption capacity could be achieved.

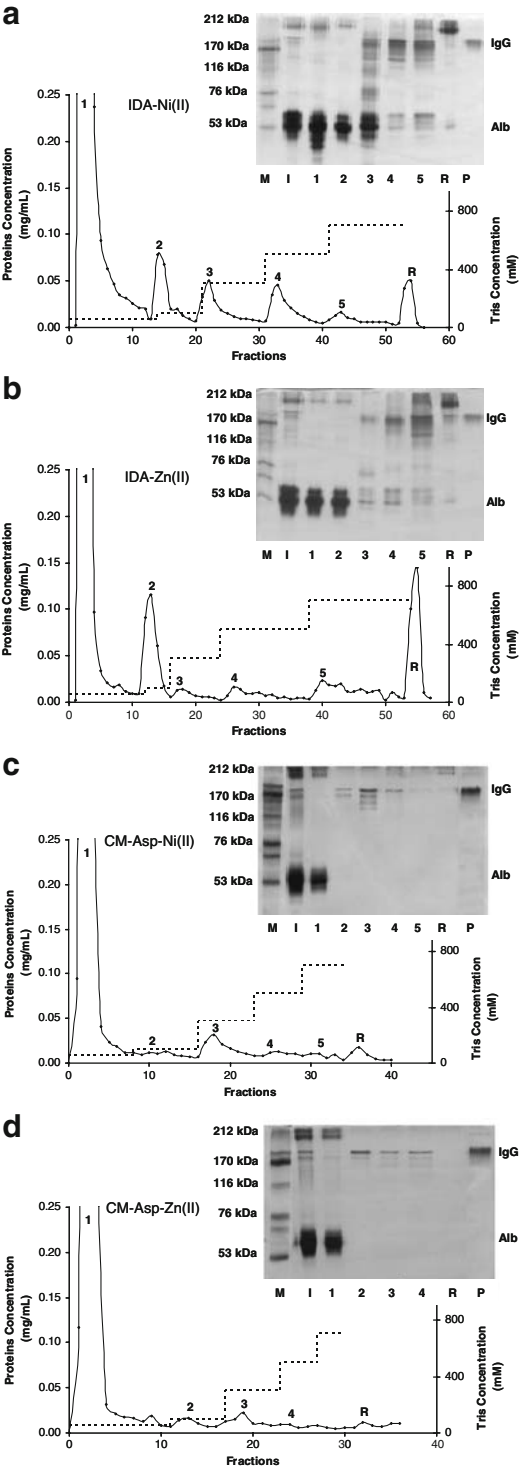

Fig. 2 Effect of the chelating ligand and metal ion on the adsorption and elution by Tris gradient of IgG_1 precipitated chromatography on **a** agarose-IDA-Ni(II), **b** agarose-IDA-Zn (II), **c** agarose-CM-Asp-Ni(II), and **d** agarose-CM-Asp-Zn(II). Adsorption buffer: Tris–HCl 50 mM, pH7.0. Dessorption: discontinuous step gradient of Tris–HCl 100, 300, 500, 700 mM, pH 7.0. Column regeneration: EDTA 50 mM, pH6.5. Other conditions: bed volume, 2.0 mL; flow rate, 0.5 mL/min; fraction volume= 3.0 mL; protein injected=2.0 mL of IgG_1 precipitate solution (about 20–30 mg of protein). Average standard deviation of protein concentrations measurement (Bradford method)=1.5%. *Insert*: SDS-PAGE analysis of fractions from the chromatography: (*M*) Molecular mass marker (GE Healthcare); (*I*) IgG_1 precipitate solution; *numbered lanes* represent aliquots of the corresponding pooled fractions of the protein peaks obtained; (*R*) pool of regeneration fractions; (*P*) human IgG (Aventis Behring)

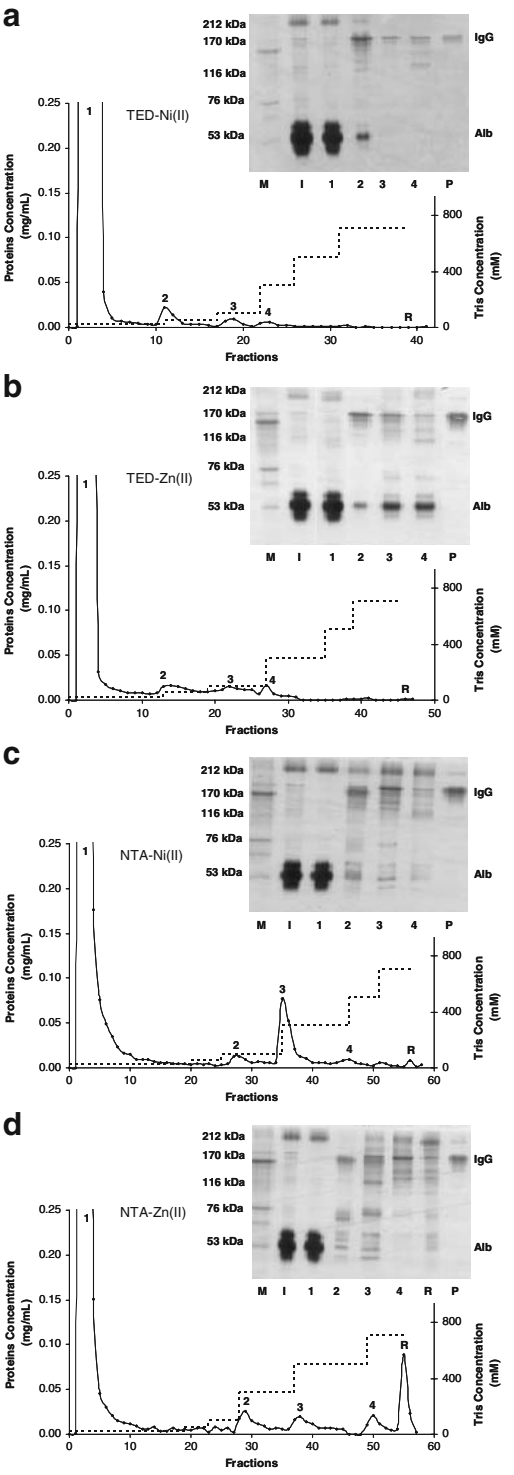

Fig. 3 Effect of the chelating ligand and metal ion on the adsorption and elution by Tris gradient of IgG_1 precipitated chromatography on **a** agarose-TED-Ni(II), **b** agarose-TED-Zn (II), **c** agarose-NTA-Ni(II), and **d** agarose-NTA-Zn(II). Adsorption buffer: Tris–HCl 25 mM, pH7.0. Dessorption: discontinuous step gradient of Tris–HCl 50, 100, 300, 500, 700 mM, pH7.0. Column regeneration: EDTA 50 mM, pH6.5. Other conditions: flow rate, 0.5 mL/min; fraction volume=3.0 mL; protein injected= 2.0 mL of IgG_1 precipitate solution (about 18–25 mg of protein); average standard deviation of protein concentrations measurement (Bradford method)=1.5%. *Insert*: SDS-PAGE analysis of fractions from the chromatography: (*M*) Molecular mass marker (GE Healthcare); (*I*) IgG_1 precipitate solution; numbered lanes represent aliquots of the corresponding pooled fractions of the protein peaks obtained; (*R*) pool of regeneration fractions; (*P*) human IgG (Aventis Behring)

Table 2 Mass balance of total protein for chromatographies of IgG_1 precipitate solution with elution by Tris–HCl step concentration gradient.

Fractions	Total protein (mg)[a]							
	IDA-Ni(II)	IDA-Zn(II)	CM-Asp-Ni(II)	CM-Asp-Zn(II)	NTA-Ni(II)	NTA-Zn(II)	TED-Ni(II)	TED-Zn(II)
Injection	21.13	17.48	11.76	10.93	18.25	18.63	19.82	23.49
Unbound fraction	18.00	15.17	11.63	10.62	17.06	18.23	22.27	21.63
Elution Tris 50 mM	–	–	–	–	0.07	0.09	0.19	0.30
Elution Tris 100 mM	0.79	0.61	0.24	0.18	0.27	0.09	0.08	0.34
Elution Tris 300 mM	0.74	0.09	0.37	0.24	0.82	0.39	0.06	0.14
Elution Tris 500 mM	0.69	0.35	0.19	0.09	0.14	0.41	0.03	0.01
Elution Tris 700 mM	0.32	0.45	0.13	0.00	0.04	0.23	0.02	0.01
Regeneration[b]	0.36	0.67	0.16	0.00	0.05	0.43	0.01	0.01
Bed volume (mL)	2.00	2.00	2.00	2.00	1.50	1.50	1.50	1.00
Adsorption capacity (mg/g of dry gel)[c]	4.39	3.30	1.65	0.78	2.82	3.33	0.70	3.15

[a] Mass calculated from protein concentration determined by Bradford [33]. Average standard deviation of Bradford method: 1.5%

[b] EDTA concentration=50 mM

[c] 1.0 mL of gel bed equals 0.33 g of dry gel

Evaluation of PEVA Membranes as Support and Comparison of PEVA-CM-Asp-Zn(II) and Agarose-CM-Asp-Zn(II)

In order to evaluate the difference in support material, chromatographic experiments were carried out in PEVA hollow fiber finely cut membranes with Ni(II) and Zn(II) chelated to CM-Asp. Results are shown in Fig. 4, and Table 3 summarizes the mass balances of these experiments.

Using atomic absorption spectrophotometry, metal-ion densities were determined, and results show that larger amounts of Ni(II) (110.6 μmol g^{-1} dry gel and 70.8 μmol g^{-1} dry membrane) than of Zn(II) (107.1 μmol g^{-1} dry gel and 51.7 μmol g^{-1} dry membrane) were chelated, independently of the support material used.

PEVA-CM-Asp-Zn(II) adsorbed about half of the amount of the total protein (0.86 mg/g of dry membrane) that was adsorbed by PEVA-CM-Asp-Ni(II) (1.55 mg/g of dry membrane) and showed a better selectivity, as is demonstrated in Fig. 4a, b. The higher capacity of PEVA-CM-Asp-Ni(II) is due to the nonspecific albumin adsorption. When these results were compared to those performed with agarose-CM-Asp, the selectivities achieved were similar.

Purification results obtained with PEVA-CM-Asp-Zn(II) showed that this procedure was efficient for obtaining MAbs enriched fractions. Elution fractions with 300 and 500 mM of Tris reached purification factors of 71.3 and 85.9, respectively, corresponding to about half of the antibodies fed into the column (according to ELISA results presented in Table 4). Concerning the purity of MAb, the SDS-PAGE analysis of fractions eluted from the PEVA-CM-Asp-Zn(II) revealed that the majority of albumin was not adsorbed by the ligand, remaining in the flowthrough.

The heavy band around 150 kDa and the bands around 100 kDa were found, by immunoblotting, to be MAb IgG_1 whole molecules and fragments (lanes 4–6, Fig. 5a) that were presented in cell culture supernatant fed solution (lane 2, Fig. 5a). IEF analysis

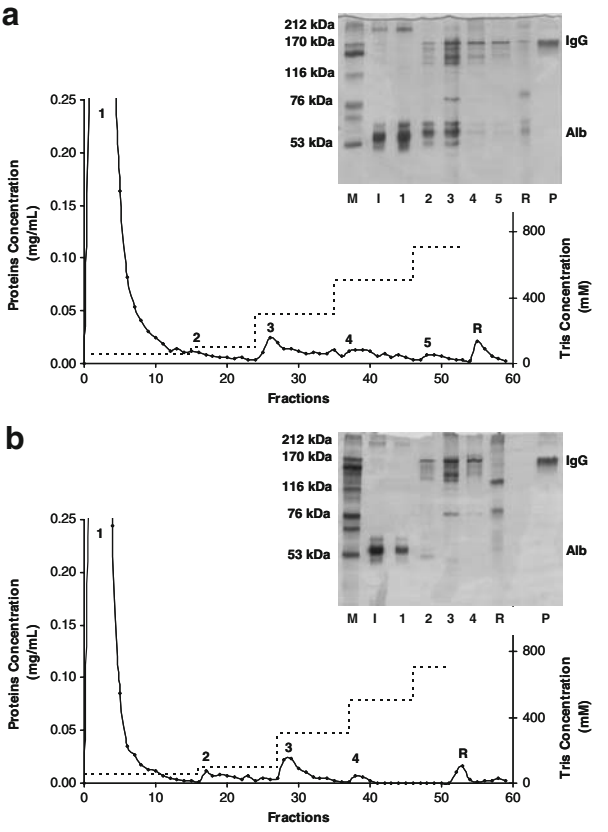

Fig. 4 Effect of the metal ion on the adsorption and elution by Tris gradient of IgG_1 precipitated chromatography on **a** PEVA-CM-Asp-Ni(II) and **b** PEVA-CM-Asp-Zn (II). Adsorption buffer: Tris–HCl 50 mM, pH7.0. Dessorption: discontinuous step gradient of Tris–HCl 100, 300, 500, 700 mM, pH 7.0. Column regeneration: EDTA 50 mM, pH6.5. Other conditions: bed volume, 5.0 mL; flow rate, 0.5 mL/min; fraction volume= 5.0 mL; protein injected= 5.0 mL of IgG_1 precipitate solution (about 60 mg of protein); average standard deviation of protein concentrations measurement (Bradford method)=1.5%. *Insert*: SDS-PAGE analysis of fractions from the chromatography: (*M*) Molecular mass marker (GE Healthcare); (*I*) IgG_1 precipitate solution; numbered lanes represent aliquots of the corresponding pooled fractions of the protein peaks obtained; (*R*) pool of regeneration fractions; (*P*) human IgG (Aventis Behring)

Table 3 Mass balance of total protein for chromatographies of IgG1 precipitate solution with elution by Tris–HCl step concentration gradient onto PEVA-CM-Asp membranes.

Fractions	Total protein (mg)[a]	
	PEVA-CM-Asp-Ni(II)	PEVA-CM-Asp-Zn(II)
Injection	61.65	61.74
Unbound fraction	54.45	58.87
Elution Tris 100 mM	0.28	0.31
Elution Tris 300 mM	0.73	0.47
Elution Tris 500 mM	0.48	0.08
Elution Tris 700 mM	0.19	0.00
Regeneration EDTA 50 mM	0.26	0.22
Bed volume (mL)	5.00	5.00
Adsorption capacity (mg/g dry membrane)[b]	1.55	0.86

[a] Mass calculated from protein concentration determined by Bradford [33]. Average standard deviation of Bradford method: 1.5%

[b] 1.0 mL of membrane bed equals 0.25 g of dry membrane. Metal-ion density: 70.8 μmol Ni(II) g^{-1} dry membrane and 51.7 μmol Zn(II) g^{-1} dry membrane

Table 4 Purification of mouse MAbs from IgG1 precipitate solution on PEVA-CM-Asp-Zn(II).

Fraction number	Total protein[a] (mg)	MAb[b] (μg)	MAb specific mass (μg MAb/mg protein)	Yield of Mab (%)[c]	Purification factor
Injection	50.82±0.76	333.3±23.33	6.6	100	1
Unbound	45.91±0.48	37.95±1.97	0.8	11.4	0.1
Elution pool (Tris 100 mM)	0.12±0.002	17.80±1.38	148.3	5.34	22.6
Elution pool (Tris 300 mM)	0.26±0.005	121.65±8.57	467.9	36.50	71.3
Elution pool (Tris 500 mM)	0.11±0.002	61.95±4.52	563.2	18.59	85.9
Elution pool (Tris 700 mM)	0.10±0.001	11.35±0.76	113.5	3.41	17.3
Regeneration (EDTA 50 mM)	0.28±0.006	3.85±0.27	13.8	1.16	2.1

[a] Dosage of protein by Bradford method [33]

[b] The amount of MAb in each fraction was determined by ELISA

[c] The yield of the MAb was determined as the ratio of the mass of MAb in the eluate fractions to the total mass of MAb present in the injected material

revealed that the eluted samples (lanes 4–6, Fig. 5b) presented a pI range from 5.85 to 7.35 similar to that of the MAb marker (obtained by the purification of the MAb using Protein-G-Sepharose, lane 7, Fig. 5b). Native PAGE presented in Fig. 5c confirmed that the procedure presented in this paper was able to purify MAbs. However, electrophoretic migration showed that the eluted antibodies were not homogeneous. When it is desirable to obtain a homogeneous preparation of MAb, an additional purification step will be required.

Pools of antibody samples from the washing, elution, and regeneration steps were analyzed by ELISA titration, seeking to evaluate a possible loss of antibody activity due to the purification process. The results showed that for all of the samples, the pools containing the IgG_1 antibodies showed positive activity up to an approximate concentration of 0.02 μg of antibody per milliliter of solution. With this result, it is possible to conclude that this purification process does not affect MAb activity, as observed by Serpa and coworkers [18] using PEVA-IDA-Zn(II).

Adsorption Isotherm Studies

In order to evaluate scale-up and thermodynamic parameters such as IgG_1 binding capacity (q_m), dissociation constant (K_d), and maximum binding energy (ΔG_{max}), adsorption isotherms were determined from experimental data obtained in batch adsorption experiments at 25°C using PEVA-CM-Asp-Zn(II) in Tris–HCl buffer 50 mM at pH7.0. The isotherm was analyzed using the Langmuir, Langmuir–Freundlich, and Temkin models (Table 5). A comparison between experimental and theoretical profiles for IgG_1 adsorption onto PEVA-CM-Asp-Zn(II) is shown in Fig. 6.

Both the Langmuir and the Langmuir–Freundlich models described the adsorption data satisfactorily (correlation coefficients of 0.998). The K_d values observed were of the order of magnitude of 10^{-6}M. These K_d values of the IgG_1-Zn(II)-CM-Asp complex indicated medium affinity, which is typical for a pseudobiospecific affinity ligand [11]. Serpa and coworkers [18] achieved a similar result for K_d, but a slightly lower q_m value of 63.4 mg g^{-1} dry membrane for the same MAb adsorption onto PEVA-IDA-Zn(II).

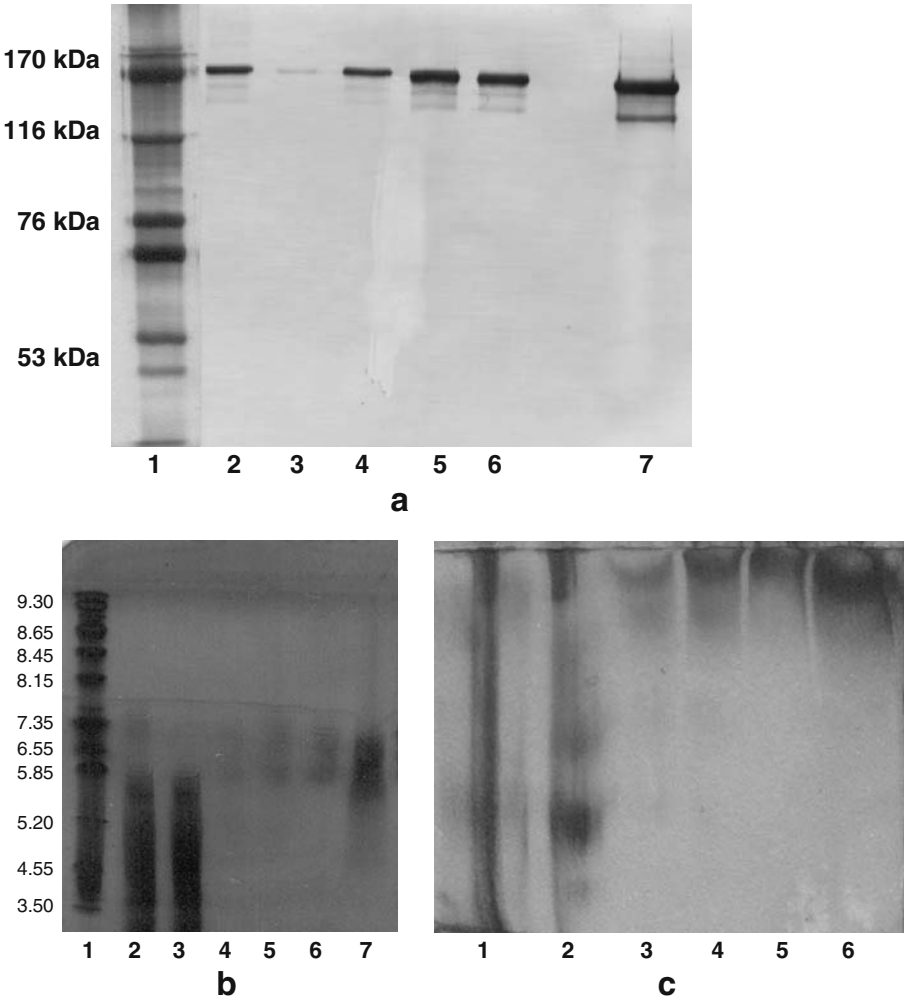

Fig. 5 Purification analysis of MAbs in PEVA-CM-Asp-Zn(II). **a** Immunoblotting; *lane 1*: Molecular mass marker of SDS-PAGE (GE Healthcare), *lane 2*: cell culture supernatant precipitated and dialyzed, *lane 3*: flowthrough, *lanes 4–6*: elution fractions at 100, 300, and 500 mM of Tris, *lane 7*: MAb marker. **b** Isoelectric focusing; *lane 1*: pI 3–9 marker (GE Healthcare), *lane 2*: cell culture supernatant precipitated and dialyzed, *lane 3*: flowthrough, *lanes 4–6*: elution fractions at 100, 300, and 500 mM of Tris, *lane 7*: MAb marker. **c** Native PAGE: *lane 1*: cell culture supernatant precipitated and dialyzed, *lane 2* flowthrough, *lanes 3–5*: elution fractions at 100, 300, and 500 mM of Tris, *lane 6*: MAb marker. The MAb marker used corresponds to purified MAb by affinity purification of the cell culture supernatant using Protein-G-Sepharose

The Langmuir–Freundlich isotherm model gave $n=1.0$, showing the absence of cooperative effects (such as attractive force due to lateral interactions), in disagreement with the results presented by Serpa and coworkers for PEVA-IDA-Zn(II) ($n=1.66$). In PEVA-IDA-Zn(II), IgG_1 molecules could bind to the matrix by multipoint interactions (IgG strong retention) or by just one metal-ion (diminishing IgG_1 adsorption capacity) or protein-protein interactions could take place [25, 39].

Table 5 Parameters of isotherm models of Langmuir, Langmuir–Freundlich, and Temkin to experimental adsorption data.

Isotherm models			
Parameters	Langmuir	Langmuir–Freundlich	Temkin
q_m (mg g^{-1} dry membrane)	77.7±1.9	77.4±3.7	–
K_d (mol L^{-1})	$(2.6\pm0.3)\times10^{-6}$	$(2.5\pm0.6)\times10^{-6}$	–
N	–	1.0±0.1	–
q_T (mg g^{-1} dry membrane)	–	–	16.9±1.7
K_T (L mol^{-1})	–	–	$(3.4\pm1.2)\times10^{6}$
ΔG_{max} (kJ mol^{-1})	–	–	−37.3
Correlation coefficient	0.998	0.998	0.993

The Temkin model, when fitted to the experimental data, also described satisfactorily the phenomenon of MAb adsorption onto PEVA-CM-Asp-Zn(II) (correlation coefficient of 0.993). The main advantage of the Temkin model is that ΔG_{max} is obtained using experimental adsorption data at only one temperature. The Temkin model was used to fit the experimental data on adsorption of human IgG onto then poly(2-hydroxyethyl methacrylate-glycidyl methacrylate) membrane (poly(HEMA-GMA)) with Cu(II) and Fe (III) chelated to L-histidine [40]. These authors achieved values of the same order of magnitude for K_T (10^6M) and ΔG_{max} (−37.6 kJ/mol). In this model, K_T is the equilibrium binding constant corresponding to the maximum binding energy.

In IMAC, the interactions between the immobilized metal ions and proteins are extremely complex in nature [26]. The interactions between IgG_1 and the immobilized metal ions could be a combined effect of electrostatic interactions, hydrophobic interaction, protein–protein, side chain, etc. and donor–acceptor (coordination) interactions of the exposed amino acid residues (such as the imidazole groups of the histidine residues) on the biomolecule surface. When a low ionic strength is used (as in this work, absence of NaCl in the adsorption buffer), the electrostatic interactions are favored withal donor–acceptor (coordination) interactions might also play a role. As indicated by the Temkin model, all these interactions would distribute the binding energies uniformly up to some maximum binding energy (ΔG_{max}). When amounts of protein adsorbed on the surface increased, the binding energy decreased. An increase in only nonspecific interactions would have the effect of decreasing q_T [39].

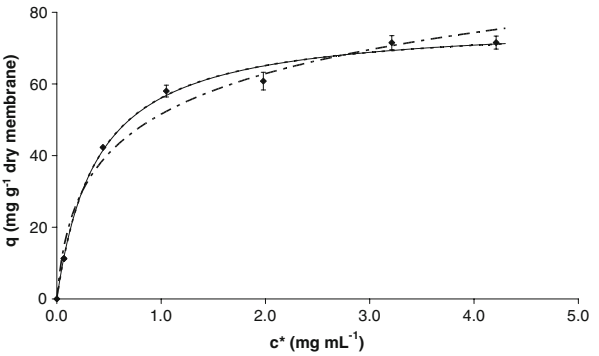

Fig. 6 Experimental adsorption isotherm (*symbol*) for anti-TNP MAb IgG_1 on PEVA-CM-Asp-Zn (II) in 50 mM Tris–HCl, pH7.0 at 25 °C. The *lines* correspond to the Langmuir model (*solid line*), the Langmuir–Freundlich model (*dotted line*), and the Temkin model (*solid–dotted line*)

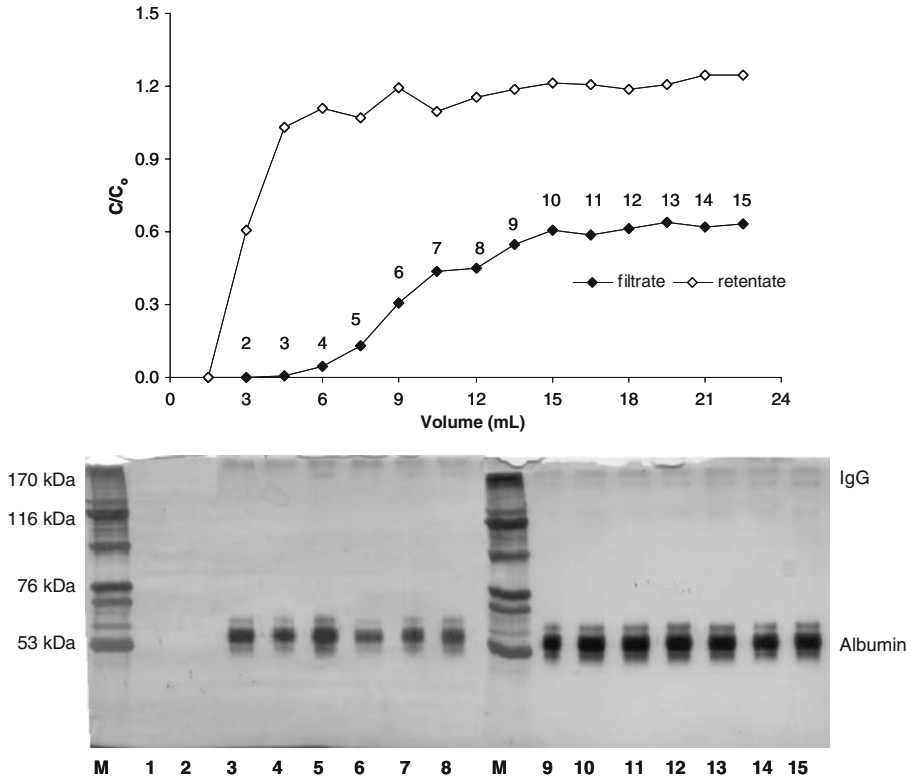

Fig. 7 Breakthrough curves of IgG_1 precipitate solution for PEVA-CM-Asp-Zn(II). SDS-PAGE analysis under nonreducing conditions of fractions of breakthrough curves. *Numbered lanes* represent aliquots of the corresponding fractions of the protein obtained at Q_F=0.5 mL/min. Lanes: (*M*) Molecular mass marker; (*1–15*) breakthrough points. Average standard deviation of protein concentrations measurement (Bradford method): 1.5%

Adsorption Breakthrough Curves Using the PEVA-CM-Asp-Zn(II) Cartridge

Protein breakthrough experiments (up to ligand saturation) were carried out with the PEVA-CM-Asp-Zn(II) cartridge. Figure 7 depicts the total protein breakthrough curves at the filtrate flow rate (Q_F) of 0.5 mL/min for IgG_1 precipitate solution on the PEVA-CM-Asp-Zn (II) cartridge. Filtrate fractions (nonretained) were analyzed by SDS-PAGE (Fig. 7).

As can be seen in the SDS-PAGE presented in Fig. 7, IgG_1 was not detected in the initial filtrate fractions (IgG_1 concentration in the filtrate was close to zero), reflecting complete adsorption of the IgG_1 molecules. As the binding sites became saturated, the breakthrough point was reached at fraction #3, corresponding to a 4.5 mL load volume. Following breakthrough, filtrate IgG_1 concentration increased and the C/C_o curve asymptotically approached values around 0.65, at which steady state was achieved in the membrane and no further protein adsorption occurred. When operating with the tangential mode of filtration, a fraction of the protein mass fed into the system was contained in the retentate and did not end up in the filtrate (C/C_o lower than unity). After the washing steps, a Tris discontinuous step gradient elution (100–700 mM at pH7.0) was performed, as can be seen in the elution profile and SDS-PAGE shown in Fig. 8.

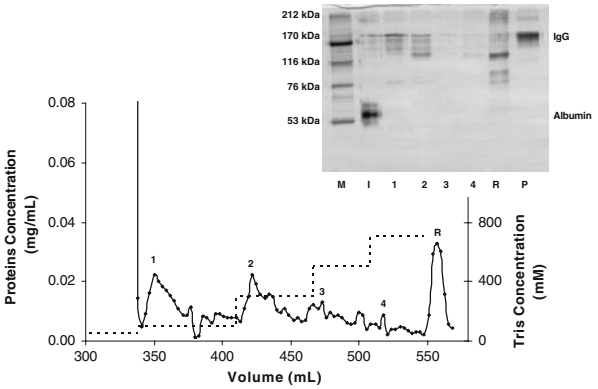

Fig. 8 Chromatographic profile obtained for the elution steps in the filtration experiments with the PEVA-CM-Asp-Zn(II) minicartridge. Adsorption and washing buffer: Tris–HCl 50 mM, pH7.0; desorption: discontinuous step gradient of Tris–HCl 100, 300, 500, 700 mM, pH7.0; regeneration: EDTA 50 mM, pH 6.5. Average standard deviation of protein concentrations measurement (Bradford method): 1.5%. *Insert*: SDS-PAGE analysis of fractions from the experiment: (*M*) Molecular mass marker; (*I*) IgG_1 precipitate solution; *numbered lanes* represent aliquots of the corresponding pooled fractions of the protein peaks obtained; (*R*) pool of regeneration fractions; (*P*) high purity IgG_1 (Aventis, Germany)

The selectivity was similar to that obtained with the PEVA-CM-Asp-Zn(II) cut fibers. The adsorption capacity of PEVA-CM-Asp-Zn(II) was 9.14 and 1.92 mg/g for the cartridge and cut fibers, respectively. This higher adsorption capacity may probably occur due to more effective activation and immobilization procedures. When the mini-cartridge derivatization was performed, the epichlorohydrin and aspartic acid solutions were forced to pass through the fibers that provided a higher immobilization of the chelating ligand and, consequently, a higher immobilization of zinc ions, making available more binding sites (128.4 μmol Zn(II) g^{-1} dry membrane).

Conclusions

We have successfully demonstrated that the PEVA-CM-Asp-Zn(II) hollow fiber membrane system is a potential alternative for the purification of monoclonal IgG_1, since the anti-TNP IgG_1 monoclonal antibodies could be adsorbed under mild conditions, close to physiological pH, and at room temperature. Different chelating ligands were tested, and CM-Asp showed promising results. A comparison with the conventional agarose bead system—agarose-CM-Asp-Zn(II)—showed a similar selectivity and capacity for the membrane configuration. A purification factor of 85.9 was achieved when the antibodies were desorbed with Tris–HCl 500 mM, pH7.0. However, membrane systems have the advantage of operating at high productivities. In contrast to the biospecific ligands commonly applied for mouse IgG_1 purification, proteins A or G, the metal chelate ligand is not at all or is to a much lesser extent subject to physical, chemical, or microbiological degradation. This facilitates considerably the handling and storage of the cartridge.

Acknowledgments The authors gratefully acknowledge the financial support of FAPESP—Fundação de Amparo à Pesquisa do Estado de São Paulo—SP, Brazil and CNPq—Conselho Nacional de Desenvolvimento Científico e Tecnológico—Brasília, DF, Brazil.

References

1. Köhler, G., & Milstein, C. (1975). *Nature, 265*, 495–497.
2. Tamashiro, W. M. S. C., & Augusto, E. F. P. (2008). Animal cell technology. In L. R. Castilho, A. M. Moraes & E. F. P. Augusto (Eds.), *From biopharmaceuticals to gene therapy* (pp. 409–434). London: Taylor & Francis.
3. Siberil, S., Dutertre, C. A., Boix, C., & Teillaud, J. L. (2005). *Transfusion Clinique et Biologique, 12*, 114–122.
4. Huse, K., Böhme, H. J., & Scholz, G. H. (2002). *J Biochem Bioph Methods, 51*, 217–231.
5. Reichert, J. M., Rosenwig, C. J., Faden, L. B., & Dewitz, M. C. (2005). *Nature Biotechnology, 23*, 1073–1078.
6. Sany, J. (2006). *C R Biologies, 329*, 228–240.
7. Walsh, G. (2006). *Nat Biotechnology, 24*, 769–778.
8. Luk, J. M., & Wong, K.-F. (2006). *Clinical and Experimental Pharmacology and Physiology, 33*, 482–488.
9. Kozlowski, S., & Swann, P. (2006). *Adv Drug Delivery Rev, 58*, 707–722.
10. Verdoliva, A., Pannone, F., Rossi, M., Catello, S., & Manfredi, V. (2002). *J Immunol Methods, 271*, 77–88.
11. Vijayalakshmi, M. A. (1989). *Trends in Biotechnology, 7*, 71–76.
12. Boschetti, E. (2001). *J Biochem Biophis Methods, 49*, 361–389.
13. Todorova-Balvay, D., Pitiot, O., Bourhim, M., Srikrishnan, T., & Vijayalakshmi, M. (2004). *J Chromatogr B, 808*, 57–62.
14. Yang, H., Gurgel, P. V., & Carbonell, R. G. (2005). *J Peptide Res, 66*, 120–137.
15. Porath, J., Carlsson, J., Olsson, I., & Belfrage, G. (1975). *Nature, 258*, 598–599.
16. Porath, J., & Olin, B. (1983). *Biochemistry, 22*, 1621–1630.
17. Vançan, S., Miranda, E. A., & Bueno, S. M. A. (2002). *Process Biochemistry, 37*, 573–579.
18. Serpa, G., Augusto, E. F. P., Tamashiro, W. M. S. C., Ribeiro, M. B., Miranda, E. A., & Bueno, S. M. A. (2005). *J Chromatogr B, 816*, 259–268.
19. Das, D., Allen, T. M., & Suresh, M. R. (2005). *Protein Expression Purif, 39*, 199–208.
20. Zimmerman, T., Frère, C. P., Satzger, M., Raba, M., Weisbach, M., Döhn, K., et al. (2006). *J Immunol Methods, 314*, 67–73.
21. Martins, S., Karmali, A., Andrade, J., & Serralheiro, M. (2006). *Molecular Biotechnology, 33*, 103–113.
22. Ribeiro, M. B., Vijayalakshmi, M., Todorova-Balvay, D., & Bueno, S. M. A. (2008). *J Chromatogr B, 861*, 64–73.
23. Platis, D., Drossard, J., Fisher, R., Ma, J. K.-C., & Labrou, N. E. (2008). *J Chromatogr A, 1211*, 80–89.
24. Ramessar, K., Rademacher, T., Sack, M., Stadlmann, J., Platis, D., Stiegler, G., et al. (2008). *Proceedings of the National Academy of Sciences, 105*, 3727–3732.
25. Gaberc-Porekar, V., & Menart, V. (2001). *J Biochem Bioph Methods, 49*, 335–360.
26. Gutiérrez, R., Martín del Valle, E. M., & Galán, M. A. (2007). *Sep Purif Reviews, 36*, 71–111.
27. Charcosset, C. (1998). *J Chem Technol Biotechnol, 71*, 95–110.
28. Tatárová, I., Gramblička, M., Antošová, M., & Polakovič, M. (2008). *J Chromatogr A, 1193*, 129–135.
29. Léo, P., Ucelli, P., Augusto, E. F. P., Oliveira, M. S., & Tamashiro, W. M. S. C. (2000). *Hybridoma, 19*, 473–478.
30. Mantovaara, T., Pertoft, H., & Porath, J. (1991). *Biotechnology and Applied Biochemistry, 13*, 315–322.
31. Bueno, S. M. A., Legallais, C., Haupt, K., & Vijayalakshmi, M. A. (1996). *J Membr Sci, 117*, 45–56.
32. El-Kak, A., & Vijayalakshmi, M. A. (1991). *J Chromatogr, 570*, 29–41.
33. Bradford, M. M. (1976). *Analytical Biochemistry, 72*, 248–254.
34. Laemmli, U. K. (1970). *Nature, 227*, 680–685.
35. Morrissey, J. H. (1981). *Analytical Biochemistry, 117*, 307–310.
36. Towbin, H., Staehelin, T., & Gordon, J. (1979). *Proceedings of the National Academy of Sciences of the United States of America, 76*, 4350–4354.
37. Chaga, G., Hopp, J., & Nelson, P. (1999). *Biotechnology and Applied Biochemistry, 29*, 19–24.
38. Hale, J. E., & Beidler, D. E. (1994). *Analytical Biochemistry, 222*, 29–33.
39. Johnson, R. D., & Arnold, F. H. (1995). *Biotechnology and Bioengineering, 48*, 437–443.
40. Bayramoglu, G., Celik, G., & Arica, M. Y. (2006). *Colloids Surf A, 287*, 75–85.
41. Yang, L., & Chen, P. (2002). *J Memb Sci, 205*, 141–153.
42. Sharma, S., & Agarwal, G. P. (2001). *Analytical Biochemistry, 288*, 126–140.